Gas sorption and transition-metal cation separation with a thienothiophene based zirconium metal–organic framework

Mostakim SK, Maciej Grzywa, Dirk Volkmer, Shyam Biswas

Angaben zur Veröffentlichung / Publication details:

SK, Mostakim, Maciej Grzywa, Dirk Volkmer, and Shyam Biswas. 2015. "Gas sorption and transition-metal cation separation with a thienothiophene based zirconium metal–organic framework." *Journal of Solid State Chemistry* 232: 221–27. https://doi.org/10.1016/j.jssc.2015.09.034.

Gas sorption and transition-metal cation separation with a thienothiophene based zirconium metal–organic framework

Mostakim SK [a], Maciej Grzywa [b], Dirk Volkmer [b], Shyam Biswas [a,*]

[a] Department of Chemistry, Indian Institute of Technology Guwahati, 781039 Assam, India
[b] Institute of Physics, Chair of Solid State Science, Augsburg University, Universitätsstrasse 1, D-86135 Augsburg, Germany

1. Introduction

Research activity on metal–organic frameworks (MOFs) [1–5] has aroused great attention in recent years. MOFs are a comparatively new type of highly crystalline and nanoporous materials. They have shown potential applications in a large variety of areas such as gas storage [6–8], chemical separation [9], catalysis [10,11] and chemical sensing [12]. They are composed of inorganic building units that are cross-linked by polytopic organic linkers. A wide variety of porous MOF structures possessing different types of pore systems (channels, cages, etc.) have been reported till date owing to the availability of a huge combination of metal ions and organic linker molecules. In sharp contrast to conventional porous adsorbents such as zeolites, mesoporous silicas, carbon nanotubes and activated carbons, the pore surface characteristics of MOFs can be changed in a systematic way by grafting various functional groups (with different sizes, polarities, acidities, hydrophilicities, etc.) to the organic linker [13–16]. The attachment of functional groups to the organic moiety can be attained by (i) using pre-functionalized [13–18] organic linkers during synthesis or (ii) employing post-synthetic modification strategy [19]. The introduction of functional groups into the MOF structures has been demonstrated to influence their sorption/separation [20,21] behavior as well as thermal and chemical stability [22,23]. Moreover, the MOFs functionalized with desired functional groups can be applied for a target application.

Sulfur (in the form of $-SO_3H$, $-SO_2-$, –SH or thiophene) containing MOFs show distinct advantages which is dependent on the nature of functional group. For example, MOFs bearing sulfonic acid groups have shown potential for proton conduction [24–28], Brønsted acid catalysis [29–31] and CO_2/CH_4 separation [15]. Sulfone-functionalized MOFs have been demonstrated to accomplish not only CO_2/CH_4 separation [32–34] but also shape-selective adsorption [35] of linear and branched alkanes. MOFs containing thiol groups have exhibited prospective for effective mercury sorption [36] and grafting of Pd(II) ions [37] for Suzuki–Miyaura coupling reactions. The potential of thienothiophene based MOFs for mercury vapor sorption [38] as well as separation [39] of transition-metal ions has been documented. However, the number of reports describing the utilities of sulfur-tagged (especially thienothiophene based) MOFs is still relatively less. It should be noted that selective transition-metal cation sorption behavior has

* Corresponding author. Fax: +91 3612582349.
E-mail address: sbiswas@iitg.ernet.in (S. Biswas).

previously been observed in a zinc MOF containing uncoordinated carboxyl groups [40], in addition to a thienothiophene-based [39] zinc MOF.

The development of MOF compounds bearing high physiochemical stability (air, water, thermal, acid–base, etc.) is a challenging goal for their applications in industry. The low physiochemical stabilities of several well-known MOF materials [41–45] have made them unsuitable for industrial applications, instead of their potential performances [8,46–50] for adsorption and separation. One strategy to synthesize MOF compounds with relatively higher physiochemical stabilities is to use transition-metal ions possessing higher oxidation states (e.g. Ti(IV) [51], Zr(IV) [52], etc.). The MOF material UiO-66 (UiO=University of Oslo) [52], which incorporates Zr(IV) ions and 1,4-benzenedicarboxylate linkers, has recently fascinated researchers with its high thermal and chemical stability as well as potential capabilities for CO_2/CH_4 gas separation [53,54]. The three-dimensional cubic framework of this compound is composed of a centric octahedral cage, which is linked with eight corner tetrahedral cages via trigonal windows. The presented thienothiophene based Zr(IV) MOF material (compound **1**) bears the same framework topology as the UiO-66 compound.

Modulators or additives have been employed for tuning the size and morphology of MOF crystals [55]. They have been used during the solvothermal synthesis of many Zr(IV) based MOF materials having UiO-66 structural topology in order to enhance their crystallinity [15,16,23,33,38,56–80]. Typically, modulators include monocarboxylic acids (e.g. benzoic acid, formic acid, acetic acid, trifluoroacetic acid, etc.), whereas additives involve water or hydrochloric acid. In this work, the thienothiophene based Zr(IV) MOF (compound **1**) has been successfully prepared in *N,N′*-dimethylformamide (DMF) by using $ZrCl_4$ as the Zr(IV) source and benzoic acid as the modulator. The influence of $ZrCl_4$/benzoic acid molar ratio on the crystallinity of compound **1** has been investigated in a systematic fashion. Herein, we wish to report on the modulated synthesis, thorough characterization, thermal and chemical stability as well as gas sorption and transition-metal cation separation properties of compound **1**. During the preparation of the manuscript, the stability and mercury vapor sorption behavior of this MOF have been reported [38]. However, the synthesis and activation routes of our compound are different. Moreover, we have studied transition-metal cation separation properties of this material.

2. Experimental

2.1. Materials and general methods

The H_2DMTDC ligand was synthesized as described previously [81]. All other starting materials were of reagent grade and used as received from the commercial suppliers. Fourier transform infrared (FT-IR) spectra were recorded in the region of 4000–440 cm^{-1} with a Perkin Elmer Spectrum Two FT-IR spectrometer. The following indications are used to characterize absorption bands: very strong (vs), strong (s), medium (m), weak (w), shoulder (sh) and broad (br). Elemental analyses (C, H, N) were carried out on a Thermo Scientific Flash 2000 CHNS-O analyzer equipped with a TCD detector. Thermogravimetric analyses (TGA) were performed with a Netzsch STA-409CD thermal analyzer in a temperature range of 25–600 °C under air atmosphere at a heating rate of 4 °C min^{-1}. Ambient temperature X-Ray diffraction (XRD) patterns were recorded on a Bruker D2 Phaser X-ray diffractometer (30 kV, 10 mA) or a Seifert XRD 3003 TT diffractometer (40 kV, 40 mA) equipped with a Meteor 1D detector and fixed divergence slits (0.5 mm), using Cu-Kα (λ=1.5406 Å) radiation. Energy dispersive X-ray (EDX) analyses were carried out with Hitachi S3400N and Zeiss Supra 55VP SEM-EDX (SEM=scanning electron microscope) instrument. Inductively coupled plasma-optical emission spectrometry (ICP-OES) experiments were performed with a Perkin Elmer Optima 5300 DV instrument. Le Bail fit of the XRD pattern of activated **1** was performed by using the Jana2006 program [82]. The nitrogen sorption isotherms were recorded using a Quantachrome Autosorb iQ-MP gas sorption analyzer at −196 °C. The carbon dioxide adsorption measurements were performed using a Belsorp Max instrument combined with a BELCryo system. Prior to the sorption experiments, the compound was degassed at 100 °C under vacuum for 24 h. It was degassed at 100 °C under vacuum for 2 h between the CO_2 sorption measurments.

The modeling of the crystal structure of compound **1** was carried out by utilizing the Materials Studio V7.0 (Accelrys Software, Inc., San Diego, CA, USA) software package. The constructed model with an artificially symmetrized version of the organic linker was refined using universal force field (UFF) molecular mechanics geometry optimization (Forcite module in Materials Studio). The constructed structure of the H_2DMTDC linker (*cf.* Fig. 2) was approximately a symmetrical overlay (without the two carboxylate groups) of the two positions of the actual linker.

2.2. Synthesis

Synthesis of $[Zr_6O_4(OH)_4(C_{10}H_6O_4S_2)_6]\cdot 4.8DMF\cdot 10H_2O$ (as-synthesized **1**): a mixture of $ZrCl_4$ (100 mg, 0.43 mmol), H_2DMTDC (110 mg, 0.43 mmol) and benzoic acid (1.57 g, 12.87 mmol) in 3 mL of DMF was heated in a sealed glass tube at 150 °C for 24 h using a block heater. After spontaneous cooling to room temperature, the white precipitate was collected by filtration, washed with acetone and dried in air. The yield was 117 mg (0.04 mmol, 60%) based on the Zr salt. Anal. calcd for $C_{74.4}H_{93.6}N_{4.8}O_{46.8}S_{12}Zr_6$: C, 32.66 H, 3.45 N, 2.46. Found: C, 32.32 H, 3.28 N, 2.37%. FT-IR (KBr, cm^{-1}): 3427 (br), 2959 (w), 2930 (w), 1661 (m), 1577 (m), 1499 (s), 1387 (vs), 1161 (m), 1119 (w), 1027 (m), 781 (m), 724 (m), 661 (s), 618 (m), and 492 (m).

2.3. Activation of the as-synthesized compound

The as-synthesized **1** was activated in two steps. In the first step, the as-synthesized compound (0.2 g) was stirred in methanol (30 mL) at room temperature for 24 h. In the second step, the white compound was collected by filtration and heated at 100 °C under dynamic vacuum for 24 h.

3. Results and discussion

3.1. Synthesis and activation

The optimized synthesis conditions for compound **1** were determined by performing solvothermal reactions of the H_2DMTDC linker with different Zr(IV) salts ($ZrCl_4$, $ZrO(NO_3)_2\cdot xH_2O$ or $ZrOCl_2\cdot 8H_2O$) in polar amide solvents like DMF, *N,N*-diethylformamide (DEF) and *N,N*-dimethylaetamide (DMA) in presence of various modulators or additives (H_2O, conc. HCl, benzoic acid, formic acid or acetic acid). As described in the Supporting information, solvothermal reactions were carried out in all possible combinations of the Zr(IV) salts, modulators/additives and amide solvents. When $ZrCl_4$ was used as the metal source and benzoic acid as the modulator in DMF, compound **1** was obtained with very high crystallinity. The $ZrCl_4/H_2$DMTDC/benzoic acid molar ratio used for achieving the optimum crystallinity was 1:1:30. The reactions in all other combinations of reactants did not yield any crystalline compound. The influence of $ZrCl_4$/benzoic acid molar

ratio on the crystallinity of compound **1** was examined in a systematic fashion. For that, the $ZrCl_4$/benzoic acid molar ratio in the reaction mixtures was tuned in the range of 1:10–1:100 (Fig. S2, Supporting information). When the reaction was performed without any benzoic acid, compound **1** possessing relatively lower crystallinity was obtained. Gradual increase in the crystallinity of the compound was noticed when the $ZrCl_4$/benzoic acid molar ratio was increased up to 1:30. The crystallinity of the compound decreased with increase in the $ZrCl_4$/benzoic acid molar ratio up to 1:50. No significant change in the crystallinity of the compound was observed with further increase in the $ZrCl_4$/benzoic acid molar ratio up to 1:100. It should be noted that the lately reported Zr-DMTDC material was prepared under solvothermal conditions (220 °C for 16 h) in DMF by using conc. HCl as an additive with a $ZrCl_4$/HCl molar ratio of 1:2 [38]. However, systematic investigation of the influence of $ZrCl_4$/HCl molar ratio on the crystallinity of the compound was not carried out.

After filtration, the as-synthesized sample of **1** was thoroughly washed with acetone for the removal of the physisorbed DMF molecules from the external surface. The removal of the guest molecules encapsulated within the pores of the compound was performed in a mild, two-step activation procedure. In the first step, the guest (H_2O and DMF) molecules entrapped within the pores were exchanged with more volatile and thus easily removable methanol molecules by stirring the as-synthesized sample in methanol. In the second step, the methanol molecules were removed from the pores by heating the methanol-exchanged sample of **1** under vacuum. The XRD patterns (Fig. 4) of the thermally activated and as-synthesized materials are very similar. This fact verifies that the compound retained its structural integrity after the activation process. It is noteworthy that the recently reported Zr-DMTDC material was activated in a similar method as that of compound **1**, except for the fact that the methanol-exchanged form of the former was achieved by Soxhlet extraction in methanol [38].

3.2. Structure description

The lattice parameters of thermally activated **1** were derived and subsequently refined from the corresponding ambient temperature XRD pattern. The unit cell parameters unambiguously suggested that compound **1** bears a cubic structure (a=23.0917 (6) Å; V=12,313.1(3) Å^3, space group=F $\bar{4}$3m). It is noteworthy that these values of the unit cell parameters matched closely with those of the recently reported Zr-DMTDC compound (a=23.12 Å; V=12,358.43 Å^3, space group=F23) [38]. Inspired by the results of unit cell determination, the cubic framework structure of compound **1** was constructed by using the Materials Studio software suite. The atomic coordinates of UiO-66 compound [83] were utilized for the construction of the structural model. Le Bail fit (Fig. 1) of the experimental XRD pattern of activated **1** resulted in good reliability factors, suggesting a good match between the experimental and calculated XRD patterns. Since compound **1** possesses the same framework topology as that of UiO-66 [38], its cubic structure (Fig. 2) is composed of hexanuclear $[Zr_6O_4(OH)_4]^{12+}$ building units. In these building units, the triangular faces of the Zr_6 octahedron are alternatively capped by μ_3–O and μ_3–OH groups. Each Zr atom, bearing a square-antiprismatic geometry, is linked with eight O atoms. One square face of the square antiprism is built up of O atoms from carboxylate groups, whereas the other square face is composed of O atoms from the μ_3–O and μ_3–OH groups. The hexanuclear $[Zr_6O_4(OH)_4]^{12+}$ building blocks are interconnected by the carboxylate groups of twelve H_2DMTDC linkers, leading to the formation of a cubic, three-dimensional framework. The network structure of **1** consists of both octahedral and tetrahedral microporous cages (Fig. 2a and b). Each octahedral cage (Fig. 2c) is surrounded by eight tetrahedral cages (Fig. 2d). The two types of cages are connected through trigonal windows. The methyl groups of the H_2DMTDC linker molecules point towards the interior of the cages.

3.3. Infrared spectroscopy

In the FT-IR spectra of the as-synthesized and thermally

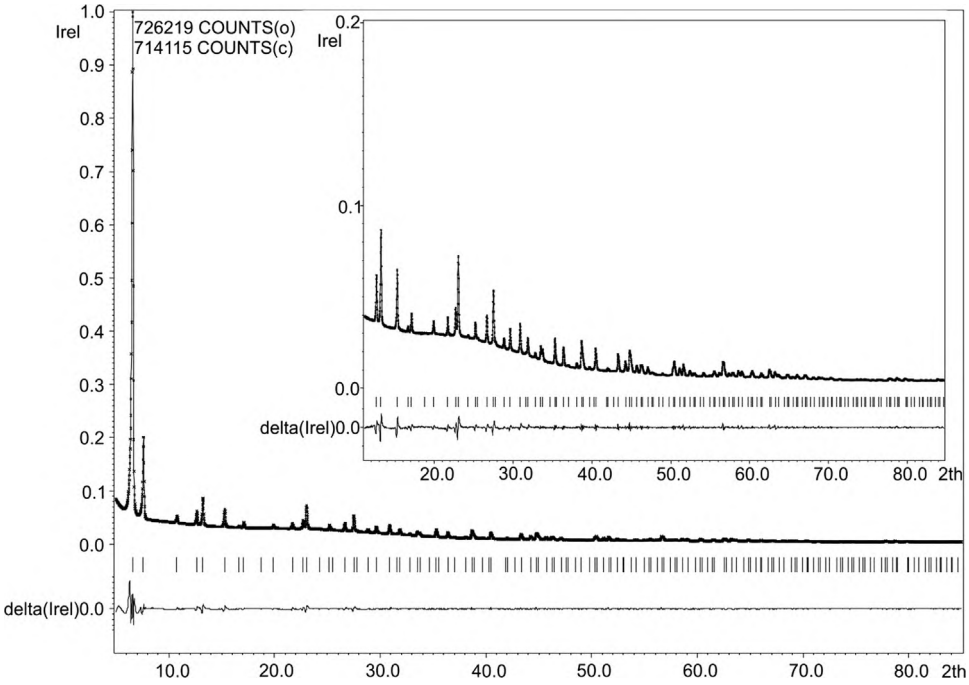

Fig. 1. Le Bail fit of the XRD pattern of thermally activated **1**. Dotted and solid lines represent observed and calculated patterns, respectively. The peak markers and the difference plot are shown at the bottom. Rp=3.33, Rwp=5.66.

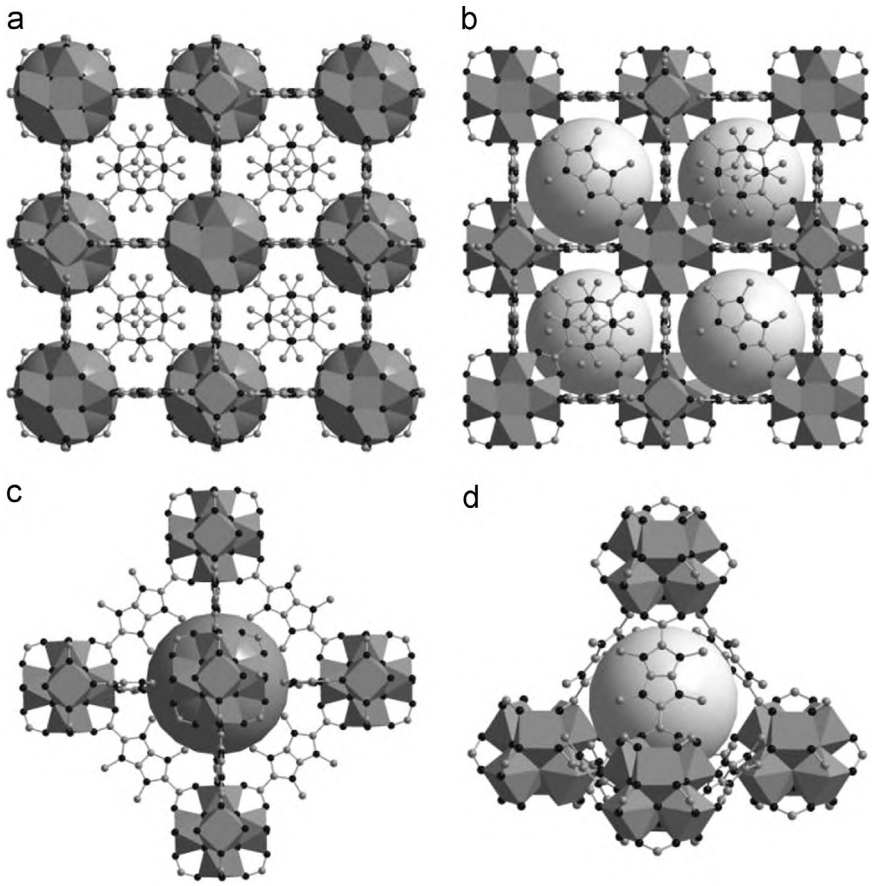

Fig. 2. (a) Ball-and-stick representation of the 3D cubic framework structure of **1**. (a, b) View of the octahedral (dark grey spheres) and tetrahedral (light grey spheres) cages in the framework. (c, d) Enlarged view of the octahedral and tetrahedral cages. Zr atoms are shown as octahedra (color codes: Zr and C, dark grey; O and S, black). The hydrogen atoms have been removed from all structural plots for clarity.

activated **1** (Fig. S1, Supporting information), the strong absorption bands at about 1570 and 1390 cm^{-1} can be assigned to the asymmetric and symmetric $-CO_2$ stretching vibrations of the coordinated DMTDC linker molecules, respectively [13,14]. The medium absorption band owing to the carbonyl stretching vibration of the occluded DMF molecules are observed at 1660 cm^{-1} in the IR spectrum of the as-synthesized **1**. The weak absorption bands at around 2860 and 2925 cm^{-1}, which are observed in the IR spectra of both as-synthesized and activated **1**, can be attributed to the C–H stretching vibrations of the $-CH_3$ groups attached with the DMTDC linker molecules [84]. In the IR spectra of the thermally activated **1**, the absorption bands owing to the guest DMF molecules are absent. This fact verifies that the material has been completely activated.

3.4. Thermal stability

Thermogravimetric analyses (TGA) were performed in an air atmosphere with the as-synthesized as well as activated samples of **1** in order to examine the thermal stability. Based on the TG analyses (Fig. 3), the as-synthesized and activated form of **1** show high thermal stability up to 310 °C. The thermal stability of **1** is slightly lower than that of the recently reported Zr-DMTDC compound having a decomposition temperature of ~350 °C [38].

In the TG curve (Fig. 3) of as-synthesized **1**, the first weight loss step of 6.8 wt% in the temperature range of 25–130 °C can be attributed to the removal of 10 occluded H_2O molecules per formula unit (calcd: 6.6 wt%). The second weight loss step of 12.7 wt%, which is observed in the temperature range of 130–310 °C, can be ascribed to the removal of 4.8 guest DMF molecules per formula

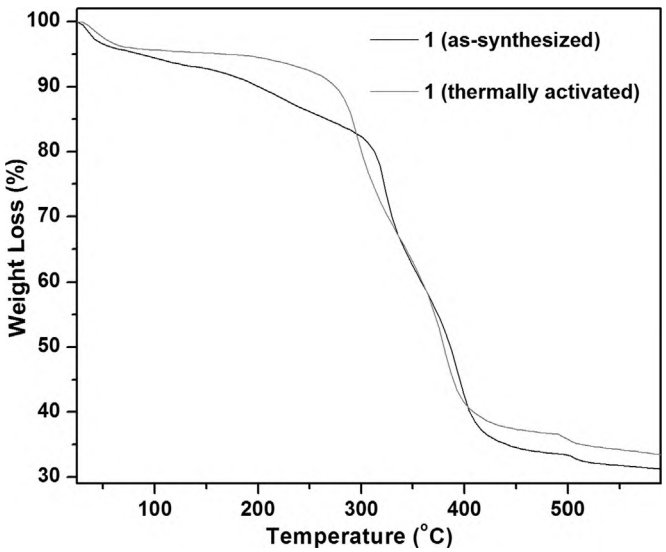

Fig. 3. TG curves of the as-synthesized (black) and thermally activated (grey) forms of **1** recorded in an air atmosphere in the temperature range of 25–600 °C.

unit (calcd: 12.8 wt%). The decomposition of the material occurs above 310 °C owing to the removal of organic linker molecules from the framework. In the TG curve of thermally activated **1**, the one weight loss step that is noticed below the decomposition temperature can be ascribed to the removal of the absorbed water molecules. This weight loss step occurs owing to the exposure of the thermally activated sample to moisture (from air) before the

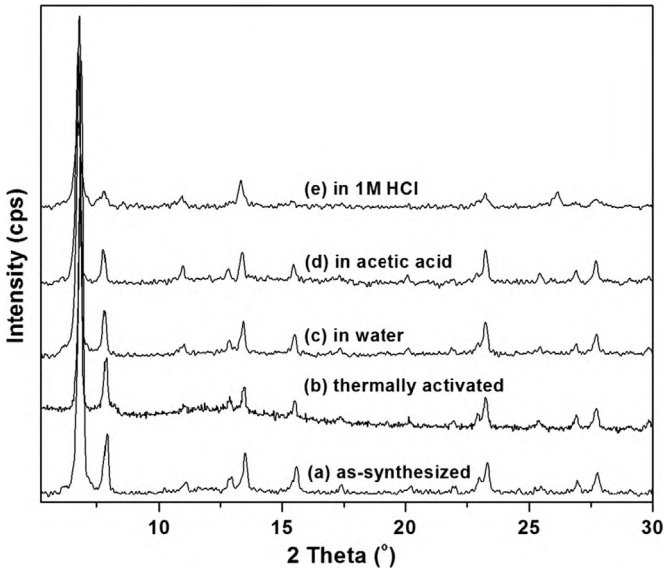

Fig. 4. XRD patterns of **1** in different forms: as-synthesized (a), thermally activated (b), treated with water (c), acetic acid (d), and 1 M HCl (e).

TG analysis, resulting in hydration of the material.

3.5. Chemical stability

For the determination of the chemical stability, the samples of thermally activated **1** were stirred in water, acetic acid, 1 M HCl and 1 M NaOH solutions for 12 h. After collection of the samples by filtration, their crystallinity were examined by XRD experiments (Fig. 4). The compound retained its crystallinity (and hence maintained its structural integrity) after treatment with water, acetic acid and 1 M HCl solutions. However, the material lost its crystallinity and became totally amorphous, after treating with 1 M NaOH solution. Thus, the stability of the material in water and acidic solutions is similar with those of the parent [52] and functionalized [15,16,22,23] UiO-66 materials as well as the recently reported Zr-DMTDC [38] compound. Nevertheless, the material showed much lower stability in basic solutions compared to the lately reported Zr-DMTDC material, which remained stable in NaOH solutions (pH = 11 and 12) for 24 h.

3.6. Gas adsorption properties

In order to investigate the extent of porosity, N_2 sorption measurements were carried out with the thermally activated form of **1**. The N_2 adsorption isotherms (Fig. 5) follow type-I behavior, which is characteristics of a microporous material. The values of the BET surface area and total pore volume were derived from the N_2 adsorption isotherms. Based on the N_2 sorption analyses, the values of BET surface area and total pore volume of activated **1** are 1236 $m^2\,g^{-1}$ and 0.68 $cm^3\,g^{-1}$ (at $p/p_0 = 0.9$), respectively. The recently reported Zr-DMTDC compound have shown BET surface area and total pore volume of 1200 $m^2\,g^{-1}$ and 0.54 $cm^3\,g^{-1}$, respectively [38]. Therefore, the values of the BET surface area and total pore volume of activated **1** are slightly higher compared to the lately reported Zr-DMTDC compound.

Low pressure CO_2 adsorption measurements were carried out with the thermally activated sample of **1** at 0 °C. The CO_2 adsorption isotherms (Fig. 6) revealed type-I behavior, which confirmed the microporous nature of the compound. The CO_2 uptake value at 0 °C and 1 bar reached as high as 3.5 mmol g^{-1}. The CO_2 adsorption capacity of activated **1** falls within the range of uptake values of other highly porous MOF materials [85,86]. The isosteric

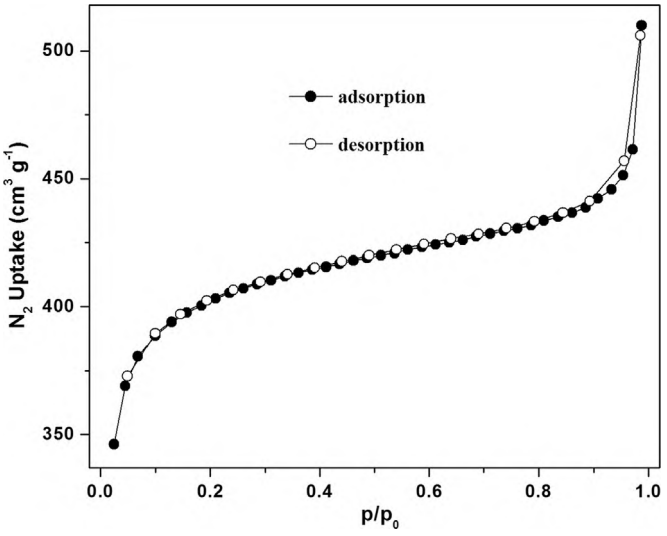

Fig. 5. N_2 adsorption (filled circles) and desorption (empty circles) isotherms of the thermally activated **1** recorded at −196 °C.

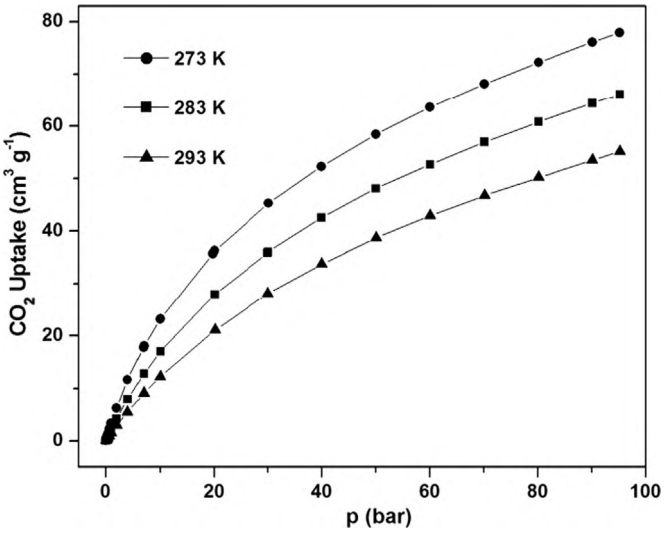

Fig. 6. CO_2 adsorption isotherms of the thermally activated **1** measured at different temperatures.

heats of adsorption (Q_{st}) values in activated **1** lie in the range of 25.5–28.1 kJ mol^{-1} depending on the degree of CO_2 loading (Fig. S3, Supporting information).

3.7. Transition-metal cation separation behavior

In order to study the transition-metal cation separation behavior, the samples (0.04 g) of thermally activated **1** were immersed at room temperature in 0.2 M solutions (10 mL in water, methanol or DMF) of transition-metal nitrates ($Co(NO_3)_2 \cdot 6H_2O$, $Ni(NO_3)_2 \cdot 6H_2O$, $Cu(NO_3)_2 \cdot 3H_2O$). After 24 h, the samples were collected by filtration, washed with copious amounts of respective solvents and dried in air. The M/Zr (M = Co, Ni or Cu) ratios were subsequently checked by EDX and ICP-OES measurements. The results of the EDX (Figs. S7–S15, Supporting information) experiments revealed that activated **1** adsorbs higher amounts of Cu^{2+} (Cu/Zr ratios: 0.087 (DMF), 0.080 (methanol), 0.047 (water)) compared to Co^{2+} (Co/Zr ratios: 6.8×10^{-3} (DMF), 0.050 (methanol), 0.017 (water)) and Ni^{2+} (Ni/Zr ratios: 7.4×10^{-3} (DMF), 0.014 (methanol), 0.023 (water)) ions, irrespective of the solvent used. The single transition-metal cation adsorption experiments

resulted in higher Cu^{2+}/Co^{2+} and Cu^{2+}/Ni^{2+} selectivity values in DMF (Cu^{2+}/Co^{2+}: 12.8, Cu^{2+}/Ni^{2+}: 11.8) as compared to those in methanol (Cu^{2+}/Co^{2+}: 1.6, Cu^{2+}/Ni^{2+}: 5.7) and water (Cu^{2+}/Co^{2+}: 2.8, Cu^{2+}/Ni^{2+}: 2.0). Similar results were also obtained from ICP-OES (Table S2, Supporting information) analyses. Thus, the nature of solvent plays a dramatic role in determining adsorption selectivity of compound **1** for transition metal ions. So far, only few MOF materials [39,40] have exhibited such selective adsorption properties for transition-metal cations. The introduction of Cu^{2+} ions into the compound can also be visualized with open eyes by the blue color (Fig. S16, Supporting information) of the $Cu(NO_3)_2$@**1** sample (treated in DMF). The XRD pattern (Fig. S17, Supporting information) of the $Cu(NO_3)_2$@**1** sample (treated in DMF) is similar to that of the thermally activated **1**, indicating that the structural integrity of **1** has been retained after incorporation of Cu^{2+} ions. Similar to the previous report [39] on Zn based MOF incorporating the DMTDC ligand, the sulfur atoms can be assigned as the possible binding sites for Cu^{2+} ions. The adsorption selectivity of activated **1** for Cu^{2+} ions over Ni^{2+} and Co^{2+} ions can be related to the different binding energies between the sulfur atoms and the transition-metal ions. Notably, the theoretical studies on the thienothiophene based Zn MOF also suggested stronger interaction energy with the framework for Cu^{2+} ions as compared to Co^{2+} ions. The solvent-dependent adsorption capacity of activated **1** for transition-metal ions might be attributed to the different solvating abilities of the tested solvents. In polar protic solvents such as water and methanol, the metal ions are strongly bound with the solvent molecules and form a sphere around the metal ions. The solvation sphere prevents coordination of the metal ions with the S atoms of the thiophene moiety of compound **1**. Thus, the material exhibits low adsorption capacities for metal ions in water and methanol. In polar aprotic solvent such as DMF, the metal ions can easily coordinate with the S atoms of the thiophene moiety of compound **1**, since solvating ability of DMF is less compared to water and methanol. Therefore, the compound shows relatively higher uptake of metal ions in DMF compared to those in water and methanol. Overall, the various binding energies between the S atoms and the transition metal ions as well as the different abilities of the solvent molecules to solvate the metal ions might be ascribed to the solvent-dependent adsorption selectivities of activated **1** for Cu^{2+} ions over Ni^{2+} and Co^{2+} ions.

4. Conclusions

The modulated synthesis, thorough characterization, gas sorption and transition-metal cation separation properties of a thienothiophene-based zirconium MOF material (compound **1**) have been demonstrated. Systematic investigations revealed that the extent of crystallinity of compound **1** is highly dependent on the $ZrCl_4$/benzoic acid molar ratio. The compound shows high thermal stability up to 310 °C in an air atmosphere, as confirmed by the thermogravimetric analyses. The remarkable chemical stability of the material in water, acetic acid and 1 M HCl solutions has been confirmed by the XRD analyses. The thermally activated **1** bears significantly high microporosity towards N_2 (S_{BET} = 1236 m^2 g^{-1}) and CO_2 (uptake = 3.5 mmol g^{-1} at 1 bar and 0 °C). Endowed with its high physiochemical stability and appreciably high microporosity, the material might develop into a potential candidate in the field of gas storage and separation. Moreover, the selective adsorption behavior of **1** for Cu^{2+} over other transition-metal ions (Ni^{2+} and Co^{2+}) might be utilized for practical transition-metal cation separation processes.

Acknowledgments

The authors acknowledge financial support from Science and Engineering Research Board (SERB; Grant no. SB/FT/CS-070/2013), New Delhi and Analytical facility from Central Instruments Facility (CIF), IIT Guwahati. We thank Ministry of Human Resource Development for Center of Excellence in FAST (Grant no. F. No. 5-7/2014-TS-VII). The authors are thankful to Mr. Dmytro Denysenko for the CO_2 sorption measurement.

Appendix A. Supplementary material

Supplementary data associated with this article can be found in the online version at http://dx.doi.org/10.1016/j.jssc.2015.09.034.

References

[1] Themed Issue on MOFs, Chem. Soc. Rev. 38 (2009) 1201.
[2] Special Issue on MOFs, Chem. Rev. 112 (2012) 673.
[3] O.M. Yaghi, M. O'Keeffe, N.W. Ockwig, H.K. Chae, M. Eddaoudi, J. Kim, Nature 423 (2003) 705.
[4] G. Férey, Chem. Soc. Rev. 37 (2008) 191.
[5] S. Kitagawa, R. Kitaura, S. Noro, Angew. Chem. Int. Ed. 43 (2004) 2334.
[6] J.R. Li, R.J. Kuppler, H.C. Zhou, Chem. Soc. Rev. 38 (2009) 1477.
[7] L.J. Murray, M. Dinca, J.R. Long, Chem. Soc. Rev. 38 (2009) 1294.
[8] L. Hamon, P.L. Llewellyn, T. Devic, A. Ghoufi, G. Clet, V. Guillerm, G. D. Pirngruber, G. Maurin, C. Serre, G. Driver, W. Van Beek, E. Jolimaitre, A. Vimont, M. Daturi, G. Férey, J. Am. Chem. Soc. 131 (2009) 17490.
[9] H. Wu, Q. Gong, D.H. Olson, J. Li, Chem. Rev. 112 (2012) 836.
[10] J. Lee, O.K. Farha, J. Roberts, K.A. Scheidt, S.T. Nguyen, J.T. Hupp, Chem. Soc. Rev. 38 (2009) 1450.
[11] L. Ma, C. Abney, W. Lin, Chem. Soc. Rev 38 (2009) 1248.
[12] L.E. Kreno, K. Leong, O.K. Farha, M. Allendorf, R.P.V. Duyne, J.T. Hupp, Chem. Rev. 112 (2012)1105 112 (2012).
[13] S. Biswas, T. Ahnfeldt, N. Stock, Inorg. Chem. 50 (2011) 9518.
[14] S. Biswas, D.E.P. Vanpoucke, T. Verstraelen, M. Vandichel, S. Couck, K. Leus, Y.-Y. Liu, M. Waroquier, V. Van Speybroeck, J.F.M. Denayer, P. Van Der Voort, J. Phys. Chem. C 117 (2013) 22784.
[15] S. Biswas, J. Zhang, Z. Li, Y.-Y. Liu, M. Grzywa, L. Sun, D. Volkmer, P. Van Der Voort, Dalton Trans. 42 (2013) 4730.
[16] S. Biswas, P. Van Der Voort, Eur. J. Inorg. Chem. (2013) 2154.
[17] T. Devic, P. Horcajada, C. Serre, F. Salles, G. Maurin, B. Moulin, D. Heurtaux, G. Clet, A. Vimont, J.-M. Greneche, B.L. Ouay, F. Moreau, E. Magnier, Y. Filinchuk, J. Marrot, J.-C. Lavalley, M. Daturi, G. Ferey, J. Am. Chem. Soc. 132 (2010) 1127.
[18] P. Horcajada, F. Salles, S. Wuttke, T. Devic, D. Heurtaux, G. Maurin, A. Vimont, M. Daturi, O. David, E. Magnier, N. Stock, Y. Filinchuk, D. Popov, C. Riekel, G. Ferey, C. Serre, J. Am. Chem. Soc. 133 (2011) 17839.
[19] K.K. Tanabe, S.M. Cohen, Chem. Soc. Rev. 40 (2011) 498.
[20] R. Custelcean, M.G. Gorbunova, J. Am. Chem. Soc. (2005) 16362.
[21] V. Colombo, C. Montoro, A. Maspero, G. Palmisano, N. Masciocchi, S. Galli, E. Barea, J.A.R. Navarro, J. Am. Chem. Soc. 134 (2012) 12830.
[22] M. Kandiah, M.H. Nilsen, S. Usseglio, S. Jakobsen, U. Olsbye, M. Tilset, C. Larabi, E.A. Quadrelli, F. Bonino, K.P. Lillerud, Chem. Mater. 22 (2010) 6632.
[23] Y. Huang, W. Qin, Z. Li, Y. Li, Dalton Trans. 41 (2012) 9283–9285.
[24] W.J. Phang, H. Jo, W.R. Lee, J.H. Song, K. Yoo, B.-S. Kim, C.S. Hong, Angew. Chem. Int. Ed. 54 (2015) 5124.
[25] P. Ramaswamy, R. Matsuda, W. Kosaka, G. Akiyama, H.J. Jeon, S. Kitagawa, Chem. Commun. 50 (2014) 1144.
[26] X.-Y. Dong, R. Wang, J.-B. Li, S.-Q. Zang, H.-W. Hou, T.C.W. Mak, Chem. Commun. 49 (2013) 10590.
[27] X.-Y. Dong, R. Wang, J.-Z. Wang, S.-Q. Zang, T.C.W. Mak, J. Mater. Chem. A 3 (2015) 641.
[28] Z. Li, G. He, Y. Zhao, Y. Cao, H. Wu, Y. Li, Z. Jiang, J. Power Sources 262 (2014) 372.
[29] J. Juan-Alcaniz, R. Gielisse, A.B. Lago, E.V. Ramos-Fernandez, P. Serra-Crespo, T. Devic, N. Guillou, C. Serre, F. Kapteijn, J. Gascon, Catal. Sci. Technol. 3 (2013) 2311.
[30] M.G. Goesten, J. Juan-Alcaniz, E.V. Ramos-Fernandez, K.B.S.S. Gupta, E. Stavitski, H.V. Bekkum, J. Gascon, F. Kapteijn, J. Catal. 281 (2011) 177.
[31] G. Akiyama, R. Matsuda, H. Sato, M. Takata, S. Kitagawa, Adv. Mater. 23 (2011) 3294.
[32] E. Neofotistou, C.D. Malliakas, P.N. Trikalitis, Chem. Eur. J. 15 (2009) 4523.
[33] P. Xydias, I. Spanopoulos, E. Klontzas, G.E. Froudakis, P.N. Trikalitis, Inorg. Chem. 53 (2014) 679.
[34] D.S. Raja, I.-H. Chang, Y.-C. Jiang, H.-T. Chen, C.-H. Lin, Microporous Mesoporous Mater. 216 (2015) 20.
[35] S. Couck, Y.-Y. Liu, K. Leus, G.V. Baron, P. Van Der Voort, J.F.M. Denayer,

Microporous Mesoporous Mater. 206 (2015) 217.
[36] K.-K. Yee, N. Reimer, J. Liu, S.-Y. Cheng, S.-M. Yiu, J. Weber, N. Stock, Z. Xu, J. Am. Chem. Soc. 135 (2013) 7795.
[37] B. Gui, K.-K. Yee, Y.-L. Wong, S.-M. Yiu, M. Zeller, C. Wang, Z. Xu, Chem. Commun. 51 (2015) 6917.
[38] K. Wang, H. Huang, W. Xue, D. Liu, X. Zhao, Y. Xiao, Z. Li, Q. Yang, L. Wang, C. Zhong, CrystEngComm 17 (2015) 3586.
[39] G.-S. Yang, Z.-L. Lang, H.-Y. Zang, Y.-Q. Lana, W.-W. He, X.-L. Zhao, L.-K. Yan, X.-L. Wang, Z.-M. Su, Chem. Commun. 49 (2013) 1088.
[40] X. Meng, R.-L. Zhong, X.-Z. Song, S.-Y. Song, Z.-M. Hao, M. Zhu, S.-N. Zhao, H.-J. Zhang, Chem. Commun. 50 (2014).
[41] L.M. Huang, H.T. Wang, J.X. Chen, Z.B. Wang, J.Y. Sun, D.Y. Zhao, Y.S. Yan, Microporous Mesoporous Mater. 58 (2003) 105.
[42] J.A. Greathouse, M.D. Allendorf, J. Am. Chem. Soc. 128 (2006) 10678.
[43] Y. Li, R.T. Yang, Langmuir 23 (2007) 12937.
[44] S.S. Kaye, A. Dailly, O.M. Yaghi, J.R. Long, J. Am. Chem. Soc. 129 (2007) 14176.
[45] D. Ma, Y. Li, Z. Li, Chem. Commun. 47 (2011) 7377.
[46] B. Wang, A.P. Cote, H. Furukawa, M. O'Keeffe, O.M. Yaghi, Nature 453 (2008) 207.
[47] L. Hamon, E. Jolimaître, G.D. Pirngruber, Ind. Eng. Chem. Res. 49 (2010) 7497.
[48] Y.-S. Bae, B.G. Hauser, O.M. Farha, J.T. Hupp, R.Q. Snurr, Microporous Mesoporous Mater. 141 (2011) 231.
[49] S. Keskin, T.M. Van Heest, D.S. Sholl, ChemSusChem 3 (2010) 879.
[50] R. Babarao, S. Dai, J. Jiang, Langmuir 27 (2011) 3451.
[51] M. Dan-Hardi, C. Serre, T. Frot, L. Rozes, G. Maurin, C. Sanchez, G. Ferey, J. Am. Chem. Soc. 131 (2009) 10857.
[52] J.H. Cavka, S. Jakobsen, U. Olsbye, N. Guillou, C. Lamberti, S. Bordiga, K. P. Lillerud, J. Am. Chem. Soc. 130 (2008) 13850.
[53] Q. Yang, H. Jobic, F. Salles, D. Kolokolov, V. Guillerm, C. Serre, G. Maurin, Chem. Eur. J. 17 (2011) 8882.
[54] Q. Yang, A.D. Wiersum, H. Jobic, V. Guillerm, C. Serre, P.L. Llewellyn, G. Maurin, J. Phys. Chem. C 115 (2011) 13768.
[55] N. Stock, S. Biswas, Chem. Rev. 112 (2012) 933.
[56] C. Zlotea, D. Phanon, M. Mazaj, D. Heurtaux, V. Guillerm, C. Serre, P. Horcajada, T. Devic, E. Magnier, F. Cuevas, G. Férey, P.L. Llewellyn, M. Latroche, Dalton Trans. 40 (2011) 4879.
[57] M.L. Foo, S. Horike, T. Fukushima, Y. Hijikata, Y. Kubota, M. Takataf, S. Kitagawa, Dalton Trans. 41 (2012) 13791.
[58] F. Vermoortele, M. Vandichel, B. Van De Voorde, R. Ameloot, M. Waroquier, V. Van Speybroeck, D.E. De Vos, Angew. Chem. Int. Ed. 51 (2012) 4887.
[59] F. Vermoortele, R. Ameloot, A. Vimont, C. Serre, D. De Vos, Chem. Commun. 47 (2011) 1521.
[60] C. Wang, Z. Xie, K.E. deKrafft, W. Lin, J. Am. Chem. Soc. 133 (2011) 13445.
[61] A. Schaate, S. Dühnen, G. Platz, S. Lilienthal, A.M. Schneider, P. Behrens, Eur. J. Inorg. Chem. (2012) 790.
[62] V. Guillerm, F. Ragon, M. Dan-Hardi, T. Devic, M. Vishnuvarthan, B. Campo, A. Vimont, G. Clet, Q. Yang, G. Maurin, G. Férey, A. Vittadini, S. Gross, C. Serre, Angew. Chem. Int. Ed. 51 (2012) 9267.
[63] A. Schaate, P. Roy, A. Godt, J. Lippke, F. Waltz, M. Wiebcke, P. Behrens, Chem. – Eur. J. 17 (2011) 6643.
[64] C. Wang, K.E. de Krafft, W. Lin, J. Am. Chem. Soc 134 (2012) 7211.
[65] S. Chavan, J.G. Vitillo, D. Gianolio, O. Zavorotynska, B. Civalleri, S. Jakobsen, M. H. Nilsen, L. Valenzano, C. Lamberti, K.P. Lillerud, S. Bordiga, Phys. Chem. Chem. Phys. 14 (2012) 1614.
[66] G. Wißmann, A. Schaate, S. Lilienthal, I. Bremer, A.M. Schneider, P. Behrens, Microporous Mesoporous Mater. 152 (2012) 64.
[67] Q. Yang, V. Guillerm, F. Ragon, A.D. Wiersum, P.L. Llewellyn, C. Zhong, T. Devic, C. Serre, G. Maurin, Chem. Commun. 48 (2012) 9831.
[68] A.D. Wiersum, E. Soubeyrand-Lenoir, B.M.Q. Yang, V. Guillerm, M.B. Yahia, S. Bourrelly, A. Vimont, S. Miller, C. Vagner, M. Daturi, G. Clet, C. Serre, G. Maurin, P.L. Llewellyn, Chem. Asian J. 6 (2011) 3270.
[69] D.A. Gomez-Gualdron, O.V. Gutov, V. Krungleviciute, B. Borah, J.E. Mondloch, J. T. Hupp, T. Yildirim, O.K. Farha, R.Q. Snurr, Chem. Mater. 26 (2014) 5632.
[70] X.-L. Lv, M. Tong, H. Huang, B. Wang, Lei Gan, Q. Yang, C. Zhong, J.-R. Li, J. Solid State Chem. 223 (2014) 104.
[71] W. Morris, B. Volosskiy, S. Demir, F. Gándara, P.L. McGrier, H. Furukawa, D. Cascio, J.F. Stoddart, O.M. Yaghi, Inorg. Chem. 51 (2012) 6443.
[72] V. Bon, V. Senkovskyy, I. Senkovska, S. Kaskel, Chem. Commun. 48 (2012) 8407.
[73] K. Manna, T. Zhang, M. Carboni, C.W. Abney, W. Lin, J. Am. Chem. Soc. 136 (2014) 13182.
[74] H. Furukawa, F. Gándara, Y.-B. Zhang, J. Jiang, W.L. Queen, M.R. Hudson, O. M. Yaghi, J. Am. Chem. Soc. 136 (2014) 4369.
[75] V. Bon, I. Senkovska, I.A. Baburin, S. Kaskel, Cryst. Growth Des. 13 (2013) 1231.
[76] B. Bueken, H. Reinsch, N. Reimer, I. Stassen, F. Vermoortele, R. Ameloot, N. Stock, C.E.A. Kirschhock, D. De Vos, Chem. Commun. 50 (2014) 10055.
[77] C. Wang, J.-L. Wang, W. Lin, J. Am. Chem. Soc 134 (2012) 19895.
[78] W. Zhang, H. Huang, D. Liu, Q. Yang, Y. Xiao, Q. Ma, C. Zhong, Microporous Mesoporous Mater. 171 (2013) 118.
[79] G. Zahn, H.A. Schulze, J. Lippke, S. König, U. Sazama, M. Fröba, P. Behrens, Microporous Mesoporous Mater. 203 (2015) 186.
[80] A. Buragohain, S. Biswas, Eur. J. Inorg. Chem. (2015) 2463.
[81] S.H. Mashraqui, H. Hariharasubrahmanian, S. Kumar, Synthesis (1999) 2030.
[82] V. Petricek, M. Dusek, L. Palatinus, Jana 2000 – The Crystallographic Computing System, Institute of Physics, Praha, Czech Republic, 2000.
[83] V. Guillerm, S. Gross, C. Serre, T. Devic, M. Bauer, G. Ferey, Chem. Commun. 46 (2010) 767.
[84] C.N. Banwell, E.M. McCash, Fundamentals of Molecular Spectroscopy, McGraw Hill, New York, 1994.
[85] K. Sumida, D.L. Rogow, J.A. Mason, T.M. McDonald, E.D. Bloch, Z.R. Herm, T.-H. Bae, J.R. Long, Chem. Rev. 112 (2012) 724.
[86] Z. Zhang, Y. Zhao, Q. Gong, Z. Li, J. Li, Chem. Commun. 49 (2013) 653.